Developmental Cell, Vol. 7, 413–424, September, 2004, Copyright ©2004 by Cell Press

# Cortical Flows Powered by Asymmetrical Contraction Transport PAR Proteins to Establish and Maintain Anterior-Posterior Polarity in the Early *C. elegans* Embryo

**Edwin Munro,[1,*] Jeremy Nance,[2] and James R. Priess[2,3]**
[1]Center for Cell Dynamics and Friday Harbor Labs
Friday Harbor, Washington 98250
[2]Division of Basic Sciences
Fred Hutchinson Cancer Research Center
Seattle, Washington 98109
[3]Howard Hughes Medical Institute
Seattle, Washington 98109

## Summary

**The *C. elegans* PAR proteins PAR-3, PAR-6, and PKC-3 are asymmetrically localized and have essential roles in cell polarity. We show that the one-cell *C. elegans* embryo contains a dynamic and contractile actomyosin network that appears to be destabilized near the point of sperm entry. This asymmetry initiates a flow of cortical nonmuscle myosin (NMY-2) and F-actin toward the opposite, future anterior, pole. PAR-3, PAR-6, and PKC-3, as well as non-PAR proteins that associate with the cytoskeleton, appear to be transported to the anterior by this cortical flow. In turn, PAR-3, PAR-6, and PKC-3 modulate cortical actomyosin dynamics and promote cortical flow. PAR-2, which localizes to the posterior cortex, inhibits NMY-2 from accumulating at the posterior cortex during flow, thus maintaining asymmetry by preventing inappropriate, posterior-directed flows. Similar actomyosin flows accompany the establishment of PAR asymmetries that form after the one-cell stage, suggesting that actomyosin-mediated cortical flows have a general role in PAR asymmetry.**

## Introduction

The ability of cells to establish and maintain polarized states is essential for numerous developmental and physiological processes. A protein complex consisting of the *C. elegans* proteins PAR-3, PAR-6, and PKC-3 has emerged as a key participant in the establishment and maintenance of cell polarities (Kemphues et al., 1988; Watts et al., 1996). These proteins, and their highly conserved counterparts in other systems, have roles in the establishment of primary embryonic axes, the establishment and/or maintenance of epithelial polarities, the directional polarities of motile cells, and the control of asymmetric cell divisions (Doe and Bowerman, 2001; Ohno, 2001; Wodarz, 2002). In all of these examples, PAR proteins are themselves localized asymmetrically. Thus an important and unresolved question is how the asymmetrical distributions of PAR proteins are established and maintained.

During the first 30 min after fertilization of the *C. elegans* egg, PAR-3, PAR-6, and PKC-3 are distributed uniformly throughout the cortex of the embryo. Shortly thereafter, these proteins become strongly enriched at the anterior cortex and are thus called the anterior PAR complex (Boyd et al., 1996; Cuenca et al., 2003; Etemad-Moghadam et al., 1995; Guo and Kemphues, 1995; Hung and Kemphues, 1999). The initial cue that determines polarity in the newly fertilized embryo is unknown, but several studies suggest that the cue is associated with the sperm centrosomes/microtubule organizing center (hereon the sperm MTOC) at the posterior pole of the embryo (Goldstein and Hird, 1996; O'Connell et al., 2000; Wallenfang and Seydoux, 2000). Localized degradation helps to determine the asymmetric distributions of some factors (e.g., germ plasm components called P-granules [Hird et al., 1996]) in the one-cell embryo. Thus one possibility is that the polarity cue triggers asymmetric degradation of the PAR proteins. However, mutations and chemical agents that affect nonmuscle myosin or actin function disrupt PAR asymmetry, suggesting that the actomyosin cytoskeleton has a crucial role in establishing and/or maintaining PAR asymmetries (Guo and Kemphues, 1996; Severson and Bowerman, 2003; Shelton et al., 1999).

The actomyosin cytoskeleton could function to anchor PAR proteins to specific cortical domains, or to exclude PAR proteins from specific cortical domains, as may occur with cortical cell fate determinants in *Drosophila* neuroblasts (Barros et al., 2003). An alternative possibility is that the actomyosin cytoskeleton actively transports PAR proteins asymmetrically (Cheeks et al., 2004; Goldstein and Hird, 1996). During the period when the PAR proteins become asymmetric, there is a profound reorganization of the cortex and cytoplasm. Local invaginations appear on the previously smooth embryo surface, suggesting an increase in surface contractility. Yolk granules near the surface begin to move anteriorly, away from the sperm MTOC, in a process called cortical flow. Yolk granules deep in the embryo begin to move posteriorly, toward the sperm MTOC, in a process called cytoplasmic flow (Hird and White, 1993; Kirby et al., 1990; Nigon et al., 1960). A brief pulse of the microfilament inhibitor cytochalasin D during the period of cortical and cytoplasmic flows causes polarity defects in wild-type embryos that mimic certain Par mutant phenotypes (Hill and Strome, 1988). Some studies on fixed embryos found a progressive accumulation of microfilaments at the anterior pole during the period of cortical and cytoplasmic flows (Kirby et al., 1990; Strome, 1986). However, these changes were not seen after fixing embryos by a different method, (Rappleye et al., 1999), or with fluorescent probes for microfilaments in living embryos (Hird, 1996). In addition, mutations in the *nop-1* gene that markedly reduce cortical furrowing and flows cause only minimal polarity defects (Rose et al., 1995).

To further investigate possible relationships between the actomyosin cortex, flows, and PAR asymmetries, we have examined the dynamics of NMY-2 (nonmuscle myosin class II heavy chain) and PAR-6 in living embryos using Green Fluorescent Protein (GFP) fusion proteins. We provide evidence that cortical flows are driven by the asymmetrical contraction of a cortical actomyosin meshwork away from the site of sperm entry, that the

*Correspondence: munroem@u.washington.edu

anterior PAR proteins are actively transported by this flow, and that PAR proteins in turn regulate the actomyosin cytoskeleton and cortical flows to promote the establishment and maintenance of PAR asymmetries. Similar flows of NMY-2 and PAR-6 accompany establishment of PAR asymmetries in subsequent embryogenesis, suggesting that actomyosin-mediated cortical transport may be a general mechanism for establishing PAR asymmetries.

## Results

The cellular events at and after fertilization have been described previously (Hird and White, 1993; Nigon et al., 1960). In brief, the sperm enters the egg at or near the future posterior pole of the embryo, and the maternal pronucleus usually is positioned at the opposite, future anterior, pole. The newly fertilized egg completes two meiotic divisions before the onset of cortical and cytoplasmic flows. Near the end of meiosis II, but prior to the onset of flows, transient small invaginations appear across the surface of the embryo. Flows initiate as the embryo completes meiosis II and the male and female pronuclei become visible. About 10 min later, a single deep invagination forms near the center of the embryo. This invagination resembles the first cleavage furrow, except that it quickly recedes and so is called the pseudocleavage furrow. Flows cease as the pseudocleavage furrow recedes and the female pronucleus migrates to meet the male pronucleus in the posterior of the embryo. After pseudocleavage, the pronuclei and associated centrosomes move as a unit to the center of the egg and rotate to align the first mitotic spindle with the long axis of the egg.

### The Actomyosin Network Is Dynamic and Symmetrical before Cortical Flows

To characterize the dynamics of the cortical actomyosin cytoskeleton, we used confocal microscopy to view embryos expressing an *nmy-2::gfp* transgene (Nance et al., 2003). Near the end of meiosis II, but prior to the onset of cortical flows, NMY-2::GFP was enriched throughout the cortex in a dynamic network of filaments and numerous dense foci (Figure 1A; Supplemental Movies S1 and S2 [http://www.developmentalcell.com/cgi/content/full/7/3/413/DC1]). Individual foci appeared to coalesce from an initially dispersed population of smaller filaments (sequence shown in Figure 1E). Once formed, foci moved short distances toward or away from one another before disappearing again, with average lifetimes of 117.9 $\pm$ 39.8 s (n = 66 foci in 3 embryos). Neighboring foci were often linked by thicker filaments that we call interfoci. Variably shaped clusters or chains of foci and interfoci often appeared to contract simultaneously, and these contractions were associated with shallow, transient invaginations in the surface of the embryo (Figure 1B and Supplemental Movie S2). These observations suggest that (1) the formation and movements of individual foci are closely associated with cortical contractions and (2) these locally contractions are mechanically coupled, forming a tensioned network throughout the cortex.

### Cortical Actomyosin Moves away from the Sperm MTOC and toward the Anterior Pole during Cortical Flow

As the embryo completes meiosis II, the sperm MTOC becomes visible in the posterior half of the embryo and moves into close association with the cortex (Goldstein and Hird, 1996; Rappleye et al., 2002). The sperm MTOC either appears and remains at the posterior pole or appears at an abaxial position before shifting to the posterior pole; this variation presumably reflects variation in the site of sperm entry (Goldstein and Hird, 1996). Regardless of its initial position, there was an immediate cessation in the formation of new NMY-2::GFP foci in the cortical region nearest the sperm MTOC. Existing foci and smaller filaments in this region moved rapidly and radially away from the sperm MTOC, generating a posterior zone devoid of foci and with a relatively smooth surface membrane (Figure 1B; Supplemental Movie S2). At the same time, foci throughout the cortex began to move toward the opposite, anterior pole at speeds up to 7.66 $\pm$ 1.0 $\mu$m/min (n = 6) (Supplemental Table S1). Local clusters or chains of foci and interfoci continued their apparent contractions while moving collectively to the anterior, generating waves of surface invaginations previously described as ruffling (Hird and White, 1993). The general, anterior movement of foci was altered in the vicinity of pronounced surface contractions, where local foci moved transiently toward the contraction. The anterior flow generated a focus-rich anterior cap and a complementary posterior clear zone containing only small, dispersed filaments (Figures 1C and 1D). Within the anterior cap, individual foci continued to coalesce, move and disappear with lifetimes similar to those seen in earlier embryos.

Within the posterior clear zone, small filaments moved toward the anterior (Figure 1F), and appeared to coalesce into new foci near the posterior rim of the anterior cap (arrow in Figure 1C). This posterior rim eventually constricted about the circumference of the egg to form the pseudocleavage furrow. Thus a local change in the assembly/disassembly dynamics of NMY-2::GFP foci near the sperm MTOC, plus a continuous flow of NMY-2::GFP-containing structures away from the sperm MTOC, results in an enrichment of NMY-2::GFP at the anterior cortex.

Previous immunostaining studies did not detect an enrichment of NMY-2 at the anterior cortex during the first cell cycle (Guo and Kemphues, 1996). We repeated these experiments using our fixation and staining conditions and found that endogenous NMY-2 was indeed distributed in the same, asymmetrical pattern we describe here for NMY-2::GFP in living embryos (data not shown). We also examined fixed wild-type embryos costained for NMY-2 and filamentous actin (F-actin), and found a close spatial correspondence between NMY-2 foci and previously described F-actin foci (Figure 1G) (Strome, 1986). Neighboring F-actin foci were typically joined by prominent F-actin containing bundles whose positions often corresponded to those of NMY-2 interfoci (Figures 1G and 1H). Like NMY-2 foci, the F-actin foci became progressively restricted into an anterior cap during cortical flows (Figures 1H–1J). Thus the dynamic events we describe for NMY-2::GFP in living embryos likely involve the entire cortical actomyosin network.

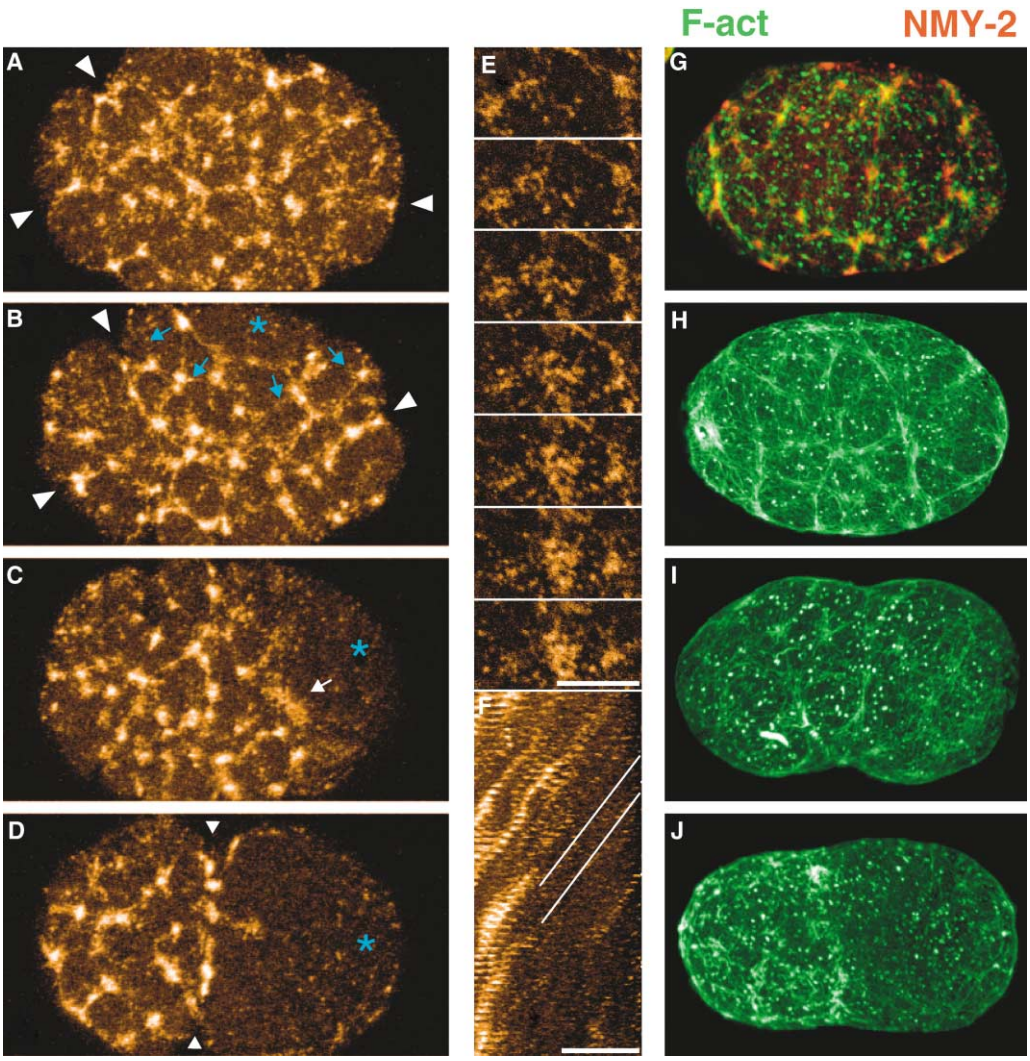


Figure 1. The Cortical Actomyosin Meshwork Flows away from the Sperm MTOC to Form an Anterior Cap

(A–D) Surface views (see Experimental Procedures) of cortical NMY-2:GFP (A) at late meiosis II (B and C), during cortical flow, and (D) at pseudocleavage. In this and subsequent figures, eggs are approximately 50 μm in length, and posterior is to the right. Blue asterisks indicate positions of the sperm MTOC. Arrowheads in (A) and (B) indicate colocalization of foci/interfoci and furrows on the egg's surface. Blue arrows (B) indicate foci moving away from the sperm MTOC. White arrow (C) indicates a new focus forming at the edge of posterior clear zone. Small white arrowheads in (D) indicate the pseudocleavage furrow.

(E) Series of frames taken at ~9 s intervals illustrating formation of a single focus.

(F) Kymograph taken from the posterior clear zone during cortical flow. White lines mark selected trajectories.

(G) Late meiosis-stage embryo costained for NMY-2 (red) and F-actin (green; yellow indicates overlap).

(H–J) Embryos stained for F-actin at late meiosis (H), during cortical flow (I), and just after pseudocleavage (J).

Scale bars = 5 μm and 10 μm in (E) and (F), respectively.

### Cortical PAR-6 and PAR-3 Form Anterior Caps during the Period of Cortical Flow

Previous studies described the progressive depletion of a PAR-6::GFP fusion protein from the posterior cortex after meiosis II (Cuenca et al., 2003), but the mechanism of depletion was unclear. We therefore used confocal microscopy to view cortical PAR-6::GFP dynamics at high resolution (Supplemental Movie S3). Just prior to the onset of cortical flows, PAR-6::GFP was enriched throughout the cortex in a diffuse layer that contained distinct punctate structures (Figure 2A). As the sperm MTOC appeared, cortical PAR-6::GFP puncta began to move away from the sperm MTOC and toward the anterior pole (Figures 2B–2E, Supplemental Movie S3). Very few puncta appeared or disappeared during cortical flow, and it was possible to track most puncta continuously for the entire flow interval. By pseudocleavage, nearly all cortical PAR-6::GFP had moved into an anterior cap whose posterior margin coincided with the pseudocleavage furrow (arrow, Figure 2C). We also observed a tight spatial correlation between NMY-2 and a second anterior PAR protein, PAR-3, in fixed embryos between meiosis II and pseudocleavage (Figure 2F and data not shown); the NMY-2 cap extended slightly posterior to the PAR-3 cap consistent with the de novo formation of NMY-2::GFP foci at the posterior. Thus PAR-6::GFP, PAR-3, F-actin, and NMY-2 all form anterior caps during the period of cortical flow.

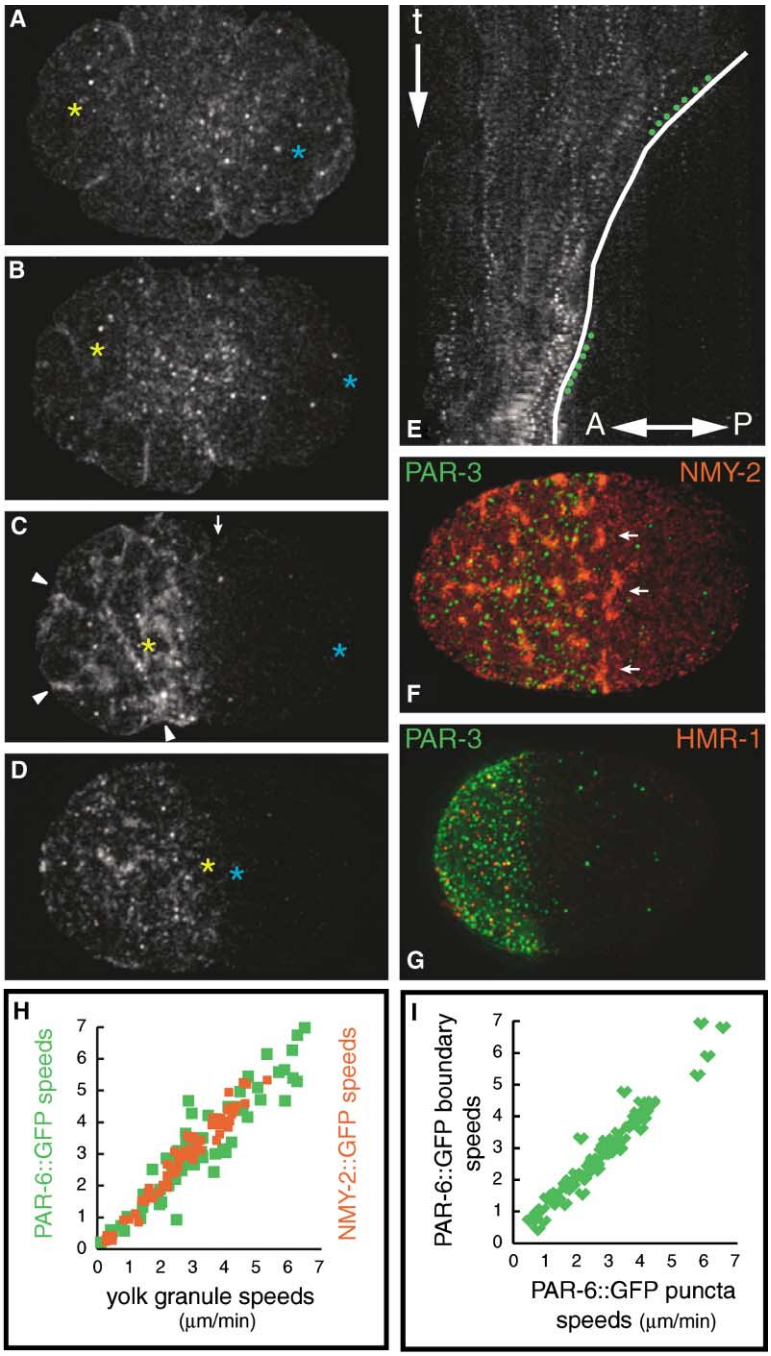


Figure 2. Cortical Transport of PAR-6::GFP Establishes an Anterior PAR-6::GFP Cap

(A–D) Surface views of PAR-6::GFP (A) at late meiosis II, (B) during cortical flow, (C) at and (D) just after pseudocleavage. In (C), arrow indicates the pseudocleavage furrow and bright linear bands of PAR-6::GFP correspond to indentations of the embryo's surface (arrowheads) that convulse actively in time-lapse movies (see Supplemental Movie S3).

(E) Kymograph analysis reveals directed posterior-anterior movements of PAR-6::GFP puncta during cortical flow. Solid line tracks the posterior edge of the PAR-6::GFP cap which moves at the same speed as PAR-6::GFP puncta (green dots).

(F) Embryo fixed during cortical flow and co-stained for NMY-2 (red) and PAR-3 (green). A posterior fringe of newly formed NMY-2 foci (arrows) extends beyond the PAR-3 domain (see text).

(G) Embryo fixed after pseudocleavage and stained for HMR-1 (red) and PAR-3 (green).

(H) Simultaneous flows of yolk granules and neighboring PAR-6::GFP puncta (green squares) or NMY-2::GFP foci (red squares).

(I) The posterior boundary of the PAR-6::GFP cap, and nearby puncta, move at the same speed.

### Cortical PAR Proteins, Actomyosin Foci, and Yolk Granules Move to the Anterior in a Common Flow

To see whether the movements of PAR-6::GFP and NMY-2::GFP described here coincide with previously described flows of subcortical yolk granules (Hird and White, 1993), we analyzed kymographs made from simultaneously acquired light and fluorescence time-lapse sequences. Neighboring PAR-6::GFP puncta and yolk granules throughout the cortex had identical speeds, as did neighboring NMY-2::GFP foci and yolk granules (Figure 2H). Therefore PAR-6::GFP puncta, NMY-2::GFP foci, and yolk granules must move within a common cortical flow. Furthermore, the PAR-6::GFP puncta located near the posterior boundary of the PAR-6::GFP cap moved at the same speed as boundary itself, suggesting that cortical flow is primarily responsible for positioning this boundary (Figures 2E and 2I).

Prior to our current study, the only non-PAR protein known to localize asymmetrically at the cortex during the period of cortical flow was the actin binding protein POD-1 that, like the PAR proteins, is essential for normal anterior-posterior polarity (Rappleye et al., 1999). Our finding that multiple components of the cortex move simultaneously toward the anterior prompted us to examine whether other cytoskeletal-associated proteins

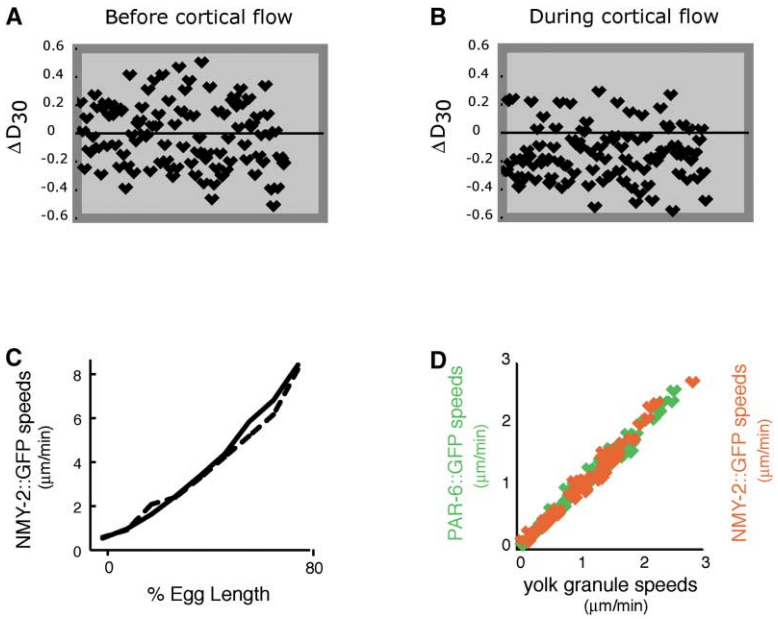


Figure 3. Myosin-Dependent Contraction Drives a Convergent Flow of Cortical NMY-2::GFP Foci, PAR-6::GFP Features, and Yolk Granules

(A and B) Relative movements ($\Delta D_{30}$) of neighboring foci throughout the cortex just before (A) and just after (B) appearance of the sperm MTOC. Negative values indicate convergence of foci.

(C) Speeds of NMY-2::GFP foci just after flow onset plotted as a function of egg length. Solid and dashed lines represent two different embryos.

(D) PAR-6:GFP (green), NMY-2::GFP (red), and yolk granules move at matching speeds in embryos partly depleted of MLC-4. Data pooled from three embryos for each probe.

might also become asymmetrically localized during cortical flow. In immunostaining experiments, we found that HMR-1/E-cadherin, HMP-2/β-catenin, and LAD-1/L1CAM each localized transiently to the anterior half of the embryo during the period of cortical flow (Figure 2G and data not shown). These results suggest that cortical flow causes a general redistribution of cytoskeletal-associated proteins to the anterior prior to pseudocleavage.

### Asymmetric Contraction of the Cortical Actomyosin Meshwork Drives Cortical Flow

We have shown: (1) that focus formation is associated with local contractions of the cortex; (2) that connections within the meshwork between adjacent foci appear to transmit local contractile forces across the cortex; and (3) that there is a local reduction in focus formation near the sperm MTOC immediately prior to the onset of flow. These results suggest that an asymmetric contraction of the entire actomyosin network away from the sperm MTOC drives cortical flow. This hypothesis makes several predictions. First, cortical flow speeds should increase monotonically from the center of the contracting domain (near the anterior pole) toward its edges (near the posterior pole; see Figure 7A). This was indeed the case (Figure 3C). Second, there should be a net convergence of neighboring foci throughout the cortex during, but not before, flow. To test this prediction, we measured the fractional change in distance between neighboring foci during 30 s intervals before and after the onset of flows ($\Delta d_{30} = d_{final} - d_{inital})/d_{initial}$). Before flow, the movements of adjacent foci were balanced; half moved together and half moved apart ($\Delta d_{30} = 0.0 \pm 0.23$; n = 100 foci in 2 embryos; Figure 3B), and the average distance between all sampled foci remained nearly the same (4.48 ± 1.09 μm versus 4.44 ± 1.01 μm). During 30 s just after the onset of flow, there was a net convergence of foci throughout the cortex; 78% moved together and 22% moved apart ($\Delta d_{30} = -0.14 \pm 0.19$; n = 100 foci in 2 embryos; Figure 3C), and the average distance between all sampled focus pairs decreased from 4.4 ± 0.98 μm to 3.76 ± 1.07 μm ($p < 0.001$; Student's paired t test).

Third, if actomyosin-based contractility is responsible for driving the coordinate flows of cortical actomyosin, PAR-6::GFP, and yolk granules, then all three of these flows should respond similarly to conditions that perturb contractility. To test this prediction, we examined PAR-6::GFP and NMY-2::GFP dynamics in embryos depleted of the regulatory myosin light chain *mlc-4* (Shelton et al., 1999). We distinguished two classes of embryos (see Experimental Procedures). Strongly depleted embryos failed both polar body extrusion and first cytokinesis. In these embryos, flows of both NMY-2::GFP and PAR-6::GFP were severely diminished, and neither of these proteins became enriched in the anterior of the embryo.(n = 4 embryos for each probe; Figures 4D–4F, Supplemental Movies S4 and S5, and data not shown). Weakly depleted embryos lacked ruffling and pseudocleavage furrows, but completed a first asymmetric division. In these embryos, cortical flows of NMY-2::GFP, PAR-6::GFP and yolk granules were attenuated (max speeds = 2.24 ± 0.2 μm/min [n = 3]), but remained closely correlated (Figure 3D), and PAR-6::GFP formed a weak cap by pseudocleavage (Supplemental Table S1). We observed similar correlations in *nop-1* embryos that lack visible signs of cortical contractility (cortical ruffling, pseudocleavage furrows) and that exhibit reduced cortical flows (Rose et al., 1995; data not shown). The coincident reduction of cortical flows of NMY-2::GFP, PAR-6::GFP and subcortical yolk granules in embryos with reduced contractility strongly supports the conclusion that myosin-based contractility drives these flows.

### The Sperm MTOC Cue Is Associated with a Local Inhibition of Contractility

If focus formation reflects local contraction of the actomyosin network and the sperm MTOC initiates cortical

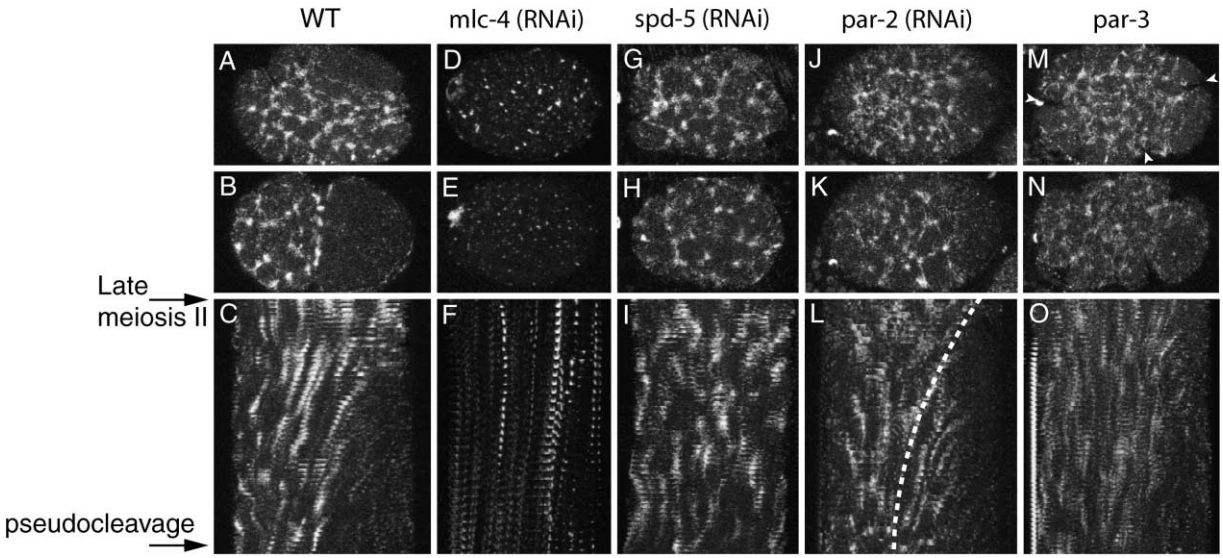


Figure 4. Cortical NMY-2::GFP Dynamics before Pseudocleavage in Mutant and RNAi-Depleted Embryos

Confocal settings were the same for all images, except (G)–(I); laser transmission = 15%, not 12%. Top rows: surface views of NMY-2::GFP near the end of meiosis II (A, D, G, J, M) and at pseudocleavage (B, E, H, K, N). Bottom row: kymographs (C, F, I, L, O) show patterns of cortical flow in the same embryos between the end of meiosis II and pseudocleavage. White arrowheads in (M) mark prominent cortical indentations that colocalize with arcs of interconnected NMY-2 foci. Dashed line in (L) track moving cortical features and to reveal the approximate extent of cortical flow.

flow by inhibiting local contractility, then local change in focal dynamics seen near the sperm pronucleus in wild-type embryos should not occur in embryos lacking a functional sperm MTOC. To test this prediction, we examined NMY-2::GFP dynamics in embryos depleted of the essential centrosomal components SPD-5 and SPD-2; these embryos lack functional centrosomes and fail to establish anterior/posterior polarity (Hamill et al., 2002; O'Connell et al., 2000). NMY-2::GFP dynamics appeared normal during late meiosis in *spd-5 (RNAi)* embryos and *spd-2* embryos. However, there was no change in NMY-2::GFP dynamics near the sperm pronucleus as it appeared and no global cortical flow of NMY-2::GFP between the end of meiosis II and pronuclear meeting (Figures 4G–4I and data not shown).

Finally, if in wild-type embryos the sperm MTOC inhibits the contractility of the local actomyosin meshwork but does not otherwise regulate flow, then network elements should all move at the same constant speed near the sperm MTOC (i.e., there should be no relative movements of neighboring elements). We examined movements of the fine, NMY-2::GFP filaments within the posterior clear zone and found that this was indeed the case (Figure 1F).

### Cortical Flows Accompany the Establishment of Later PAR Asymmetries

If asymmetric contraction of cortical actomyosin is a general mechanism for establishing PAR asymmetries, then coordinate flows of NMY-2::GFP and PAR-6::GFP should be associated with other PAR asymmetries in the early embryo. After the one-cell stage, early embryonic cells exhibit one of two distinct patterns of PAR asymmetry. The lineage of embryonic cells that ultimately produces the germline executes a sequence of asymmetrical divisions analogous to the first division of the embryo, and each of these germline precursors shows anterior localization of PAR-3, PAR-6, and PKC-3 prior to division (Etemad-Moghadam et al., 1995; Hung and Kemphues, 1999). We examined NMY-2::GFP and PAR-6::GFP in the first germline precursor (the P1 cell) and observed an anterior cortical flow of both proteins (Figure 5A; Supplemental Movies S6 and S7). NMY-2::GFP and PAR-6::GFP flows occurred at similar speeds and resulted in the formation of anterior NMY-2::GFP and PAR-6::GFP caps within the P1 cell (Figures 5B–5D; the dotted line in Figure 5B spans P1).

Beginning late in the four-cell stage, embryonic cells that do not form the germline develop an apicobasal PAR asymmetry. The former "anterior" PAR proteins PAR-3, PAR-6, and PKC-3 localize to the apical, contact free surface of a cell, while the former "posterior" PAR protein PAR-2 localizes to basal/lateral surfaces that contact other cells (Etemad-Moghadam et al., 1995; Boyd et al., 1996; Hung and Kemphues, 1999; Nance and Priess, 2002). As predicted, we detected prominent cortical flows of NMY-2::GFP and PAR-6::GFP in the somatic precursors of eight-cell stage embryos. The flows began during interphase, and were directed toward the apical, contact-free surface (Figures 5E–5H; Supplemental Movies S8 and S9). We conclude that cortical flows are associated with all examples of PAR asymmetry in the early embryo.

### Anterior PAR Proteins Regulate Actomyosin Dynamics and Cortical Flow

Previous studies showed that the anterior PAR protein *par-3* is required for cytoplasmic flows and formation of

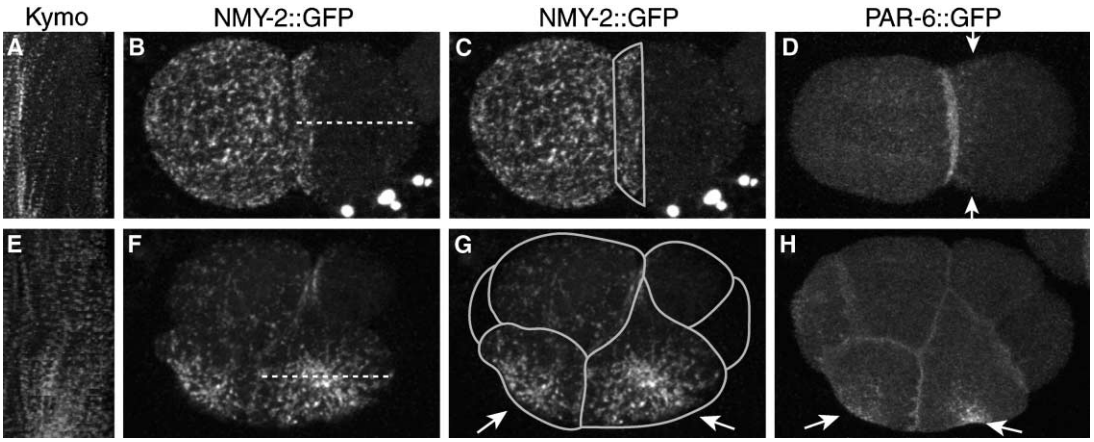


Figure 5. Cortical Flows in Later Embryos

(A–D) Two-cell stage. NMY-2::GFP (B and C) and PAR-6::GFP (arrows in [D]) accumulate at the anterior of P1 (cell on right). PAR-6::GFP also accumulates at high levels at the site of cell-cell contact. Kymograph in (A) shows cortical flow of NMY-2::GFP into this domain.

(E–H) Eight-cell stage. NMY-2::GFP (F and G) and PAR-6::GFP (H) accumulate within apical caps of AB cells (arrows in [G] and [H]). Kymograph in (E) shows cortical flow of NMY-2::GFP into this cap.

an anterior F-actin cap (Kirby et al., 1990). We therefore asked whether actomyosin organization and dynamics were altered in embryos lacking anterior PAR proteins. Near the end of meiosis in *par-3* mutant embryos, the cortical NMY-2::GFP network resembled that of wild-type embryos, and numerous invaginations covered the embryo's surface (Figure 4M). As the sperm MTOC formed, extant foci moved rapidly away from the cortical point nearest the MTOC, generating a small clear zone similar to that of wild-type embryos (Figures 4M and 4N). However, the collective flow of foci away from the clear zone was greatly attenuated compared to that of wild-type embryos, such that an abnormally large anterior cap of NMY-2::GFP persisted until pseudocleavage ($n = 10$; cap size $= 80 \pm 2\%$; $n = 6$; Figures 4M–4O; Supplemental Table S1; and Supplemental Movie S10). Also, the relative movements of neighboring foci within the anterior cap were severely diminished during the period of cortical flow (absolute value of $\Delta$d30 ($|\Delta d30|$) $= 0.08 \pm 0.07$ compared to the wild-type $|\Delta d30| = 0.2 \pm 0.13$). We observed similar phenotypes in embryos depleted of PAR-3, PAR-6, or PKC-3 by RNAi (data not shown). Together, these data suggest that the posterior cue remains active in embryos lacking anterior PAR proteins, but the *net* forces responsible for moving foci relative to one another and toward the anterior pole in response to this cue are reduced (see Discussion). The basis for this reduction remains unclear. However, *par-3* embryos depleted of either PAR-2 or PAR-1 by RNAi exhibited defects in the movements of cortical foci similar to those seen in *par-3* alone (data not shown), suggesting that the defects observed in *par-3* embryos are not due to the ectopic localization of PAR-2 or PAR-1.

### PAR-2 Inhibits the Posterior Cortical Recruitment of NMY-2 after Pseudocleavage to Maintain PAR Asymmetries

As PAR-3, PAR-6, and PKC-3 move to the anterior during cortical flows, PAR-2 localizes to a complementary posterior cortical domain. Previous studies showed that PAR-2 is not required to establish anterior PAR asymmetries before pseudocleavage, but is required to maintain them between pseudocleavage and first cleavage (Cuenca et al., 2003). Consistent with these observations, we detected only minor defects in the cortical flow of NMY-2::GFP before pseudocleavage in *par-2 (RNAi)* embryos (Figures 4J–4L; Supplemental Table S1; Supplemental Movie S11): Anterior flow speeds fell off more rapidly toward the anterior than in the wild-type (Figure 4L; Supplemental Table S1) and the rate at which new foci formed near the rear edge of the anterior cap was approximately twice that in wild-type embryos, resulting in a broader than normal NMY-2::GFP cap (Figures 4J and 4K). But the magnitude of cortical flow was sufficient to account for the establishment of a normally positioned anterior PAR-6::GFP domain by pseudocleavage (Figure 4L; Supplemental Table S1; but see also Cheeks et al., 2004).

In contrast, we observed marked differences between wild-type embryos and PAR-2-depleted embryos in localization and dynamics of NMY-2::GFP and PAR-6::GFP between pseudocleavage and first cleavage. In wild-type embryos after pseudocleavage, NMY-2::GFP foci disappeared, and an anterior cap of fine NMY-2::GFP fibers formed in their place and persisted until metaphase (Figures 6A and 6B and Supplemental Movie S2). During this interval, we observed anterior-directed flows of cortical myosin terminating in a dense band at the posterior edge of the anterior NMY-2::GFP cap (Figures 6A and 6B); analysis of fixed, stained embryos showed that this dense band of NMY-2 corresponded to a gap between anterior-localized PAR-3 and posterior-localized PAR-2 (Figures 6G–6L). By contrast, in *par-2 (RNAi)* embryos, the disappearance of anterior NMY-2::GFP foci was followed by formation of a dense network of NMY-2::GFP fibers over most of the cortex (Figure 6C; Supplemental Movie S11). The appearance of posterior, ectopic NMY-2::GFP fibers was associated with a pronounced, posterior-directed cortical flow of NMY-2::GFP (Figure 6D; Supplemental Movie S11) and a concurrent flow of PAR-6::GFP (Figure 6F; Supplemental

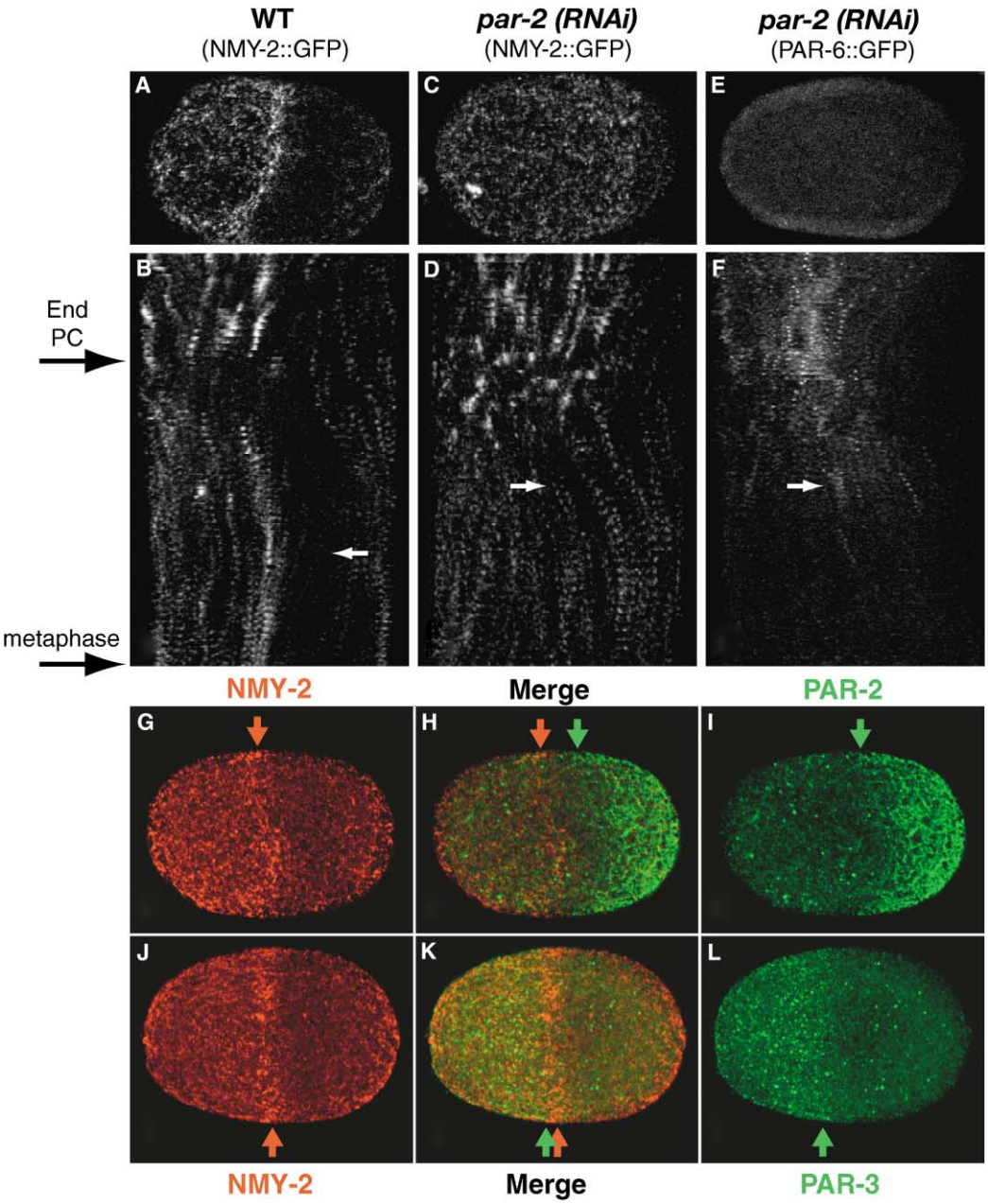


Figure 6. Cortical NMY-2 Flows and Maintenance of PAR Distributions after Pseudocleavage

(A–F) Cortical flows of NMY-2::GFP and PAR-6::GFP in wild-type and *par-2 (RNAi)* embryos. (A, C, and E) Surface views of metaphase stage embryos. (B, D, and F) Kymographs from the same embryos. Arrow in (B) shows the anterior flow of NMY-2::GFP into a dense band at the rear edge of the anterior cap. In *par-2 (RNAi)* embryos, aberrant posterior flows of NMY-2::GFP and PAR-6::GFP (arrows in [D] and [F]) return these proteins to the posterior cortex (C and E).

(G–L) Embryos fixed at metaphase and costained for NMY-2 and PAR-2 (G–I) or NMY-2 and PAR-3 (J–L).

Movie S12). This aberrant flow was sufficient to redistribute PAR-6::GFP to the posterior cortex by metaphase (Figures 6E and 6F). These observations suggest that PAR-2 functions in wild-type embryos to inhibit NMY-2 from accumulating at the posterior cortex and thus prevents abnormal flows after pseudocleavage that would otherwise redistribute anterior PAR proteins to the posterior cortex. Consistent with this hypothesis, we found that *par-3* mutants with uniformly distributed PAR-2 showed low, uniform levels of cortical NMY-2::GFP after pseudocleavage (Supplemental Movie S10), while *par-3;par-2(RNAi)* embryos lacking PAR-2 had high, uniform levels of cortical NMY-2::GFP (data not shown).

## Discussion

Our observations, together with many previous results, form the core of a working hypothesis for how PAR proteins might interact with one another and with a contractile actomyosin cortex to form and stabilize cortical

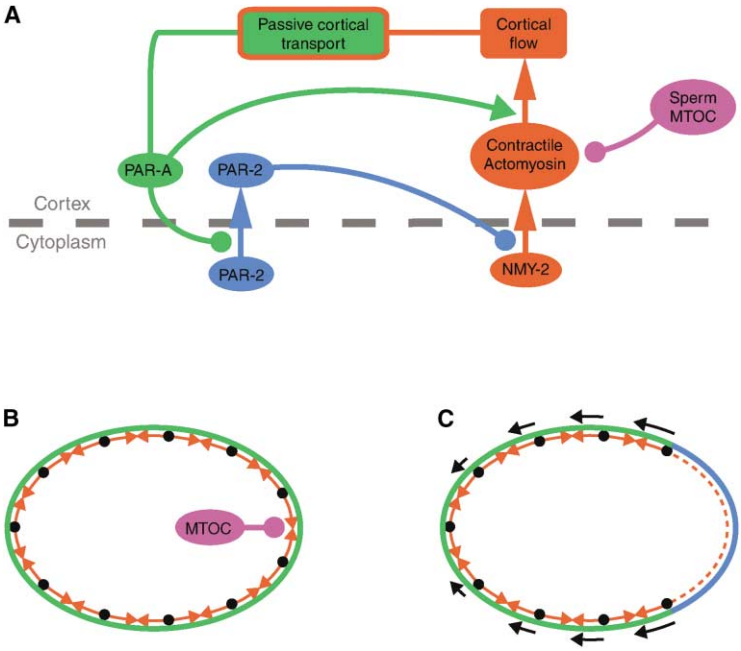


Figure 7. Model for the Establishment and Maintenance of PAR Domains

(A) A network of interactions among PAR proteins, the cortical actomyosin cytoskeleton, and the sperm MTOC in the one-cell *C. elegans* embryo.

(B and C) Dynamic consequences of these network interactions during the establishment/maintenance of AP polarity. A signal from the sperm MTOC weakens the cortex locally causing a posterior-directed cortical flow that transports PAR-3, PAR-6, and PKC-3 to the anterior. PAR-3, PAR-6, and PKC-3 modulate cortical actomyosin dynamics to promote cortical flow and their own transport. Depletion of PAR-3, PAR-6, and PKC-3 from the posterior cortex removes an inhibitory influence that leaves PAR-2 free to accumulate there. Cortical PAR-2 in turn inhibits the cortical accumulation of NMY-2 on the posterior cortex. This reinforces the sperm cue during the establishment phase, prevents an aberrant posterior flow of NMY-2 and PAR-3, PAR-6, and PKC-3 after pseudocleavage, and may promote the contractile retention of PAR-3, PAR-6, and PKC-3 during the maintenance phase.

PAR domains in response to a localized signal from the sperm MTOC (Figure 7). We discuss the elements of the hypothesis below.

### Cortical Flows Are Driven by the Asymmetrical Contraction of a Dynamic Actomyosin Network

White and colleagues (White and Borisy, 1983; Bray and White, 1988) proposed how a local modulation of global cortical contractility could produce tension gradients in the cortex that would drive flows of cortical cytoplasm away from regions of low cortical tension and toward regions of high cortical tension. More specifically, Hird and White (1993) hypothesized that cortical flows in the one-cell *C. elegans* embryo might be caused by a local relaxation of cortical tension through an interaction between the sperm MTOC and the cortex. Our results support this idea and reveal the cytoskeletal basis for contractile force generation and cortical flow: prior to the appearance of a distinct sperm pronucleus, F-actin and NMY-2 constitute a dynamic network of short-lived foci that form through transient local, myosin-dependent, contractions of the cortical meshwork. The association of surface invaginations with groups of foci and interfoci and the evident continuity of the actomyosin meshwork (Figures 1G–1J) implies that neighboring foci are mechanically coupled to form a network of tensioned elements. Prior to appearance of the sperm MTOC, local contractions associated with focus formation drive small transient displacements of foci, but the network is globally stable. Appearance of the sperm MTOC is associated with an immediate, local cessation of focus formation, reflecting an apparent diminution of contractility or weakening of the otherwise symmetrical actomyosin network. The resulting global tension imbalance should cause an immediate and collective flow of remaining foci toward one another and away from the sperm MTOC as the entire meshwork contracts asymmetrically toward the opposite, anterior pole. Our measurements of focus movements before and after appearance of the sperm MTOC confirm this prediction, and the loss of convergent flow in embryos lacking the regulatory myosin light chain MLC-4 confirms the contractile basis for these flows.

How do flows continue once initiated? Our observations reveal a continuous local cycle of focus assembly/contraction followed by disassembly. The local contractions that produce each individual focus are short-lived, but at any time during flow, these contractions are distributed throughout the anterior cap and coupled to one another to form a continuously tensioned network. Thus the cortex appears to be a self-renewing contractile engine that continues to generate tension even as it contracts, rather than a pre-tensioned network that contracts once to release stored tension. Likewise, the persistent absence of foci in the posterior clear zone, and the constant flow speeds of filaments away from this zone, suggest a continued absence of contractility near the sperm MTOC. Thus, sustained, asymmetrical contractile force generation appears to sustain a continued cortical flow.

Previous studies suggest that factors closely associated with the sperm MTOC supply the cue that initiates cortical flow in the one-cell embryo, although the relative importance of the centrosome itself and the sperm astral microtubules remains controversial (Goldstein and Hird, 1996; Hird and White, 1993; O'Connell et al., 2000; Sonneville and Gonczy, 2004; Wallenfang and Seydoux, 2000). Our observations that focus dynamics remain unchanged near the newly formed sperm pronucleus, and that cortical flows never initiate in embryos depleted of essential centrosomal components (which also lack a sperm aster), support this hypothesis. Furthermore, they suggest that the sperm cue acts by modulating the actomyosin contractility cycle to produce a local

reduction of cortical tension. Discovering the nature of this modulation is an important future goal.

### Cortical Transport of the Anterior PAR Complex Establishes an Anterior PAR Domain during Pseudocleavage

We have shown that NMY-2::GFP foci, PAR-6::GFP puncta, and yolk granules each move toward the anterior pole at the same velocity, indicating that all are components of the same cortical flow. Our observation that the rear boundary of the anterior PAR-6 cap moves at the same speed as this flow (see also Cheeks et al., 2004) suggests that cortical transport is the dominant mechanism for establishing an anterior PAR domain. Several lines of evidence suggest that the other members of the anterior PAR complex, PAR-3 and PKC-3, localize through the same cortical flow. PAR-3, PAR-6, and PKC-3 colocalize extensively in coimmunostaining experiments (Hung and Kemphues, 1999; Nance et al., 2003; Tabuse et al., 1998; Watts et al., 1996), and our analysis of fixed embryos showed coincident distributions of NMY-2 and endogenous PAR-3. PAR-3 and PKC-3 are both essential for the cortical localization of PAR-6 (Tabuse et al., 1998; Nance et al., 2003; Watts et al., 1996), and homologs of these proteins can complex in vitro (Joberty et al., 2000; Lin et al., 2000). PAR-3 appears to provide the critical link that enables PAR-6 and PKC-3 to associate with the cortex, since it is the only member of the complex that can localize cortically in the absence of the others (Hung and Kemphues, 1999; Tabuse et al., 1998; Watts et al., 1996, Nance et al., 2003). PAR-3 is unlikely to bind NMY-2 directly as it remains associated with the cortex when NMY-2 is depleted from the embryo (Guo and Kemphues, 1996). However, PAR-3 cortical localization may involve actin or actin binding proteins since depleting cortical F-actin prevents PAR-3 from associating with the cortex (Severson and Bowerman, 2003).

We also found that the non-PAR proteins HMR-1/E-Cadherin, HMP-2/β-catenin, and LAD-1/L1CAM each localize to the anterior pole of the embryo during cortical flow. None of these proteins have a known role in early embryonic polarity, but they or their homologs in other animals can associate indirectly with the cortical actin cytoskeleton (Chen et al., 2001; Costa et al., 1998). Thus cortical flow at the one-cell stage may be a feature common to all proteins associated with the actomyosin cytoskeleton.

### Cortical Flows and PAR Asymmetry after the One-Cell Stage

We have shown that coordinate flows of NMY-2 and PAR-6 are associated with multiple examples of cortical PAR asymmetry in the early *C. elegans* embryo. This suggests that asymmetrical contractile flows underlie each asymmetry, although the cues that initiate these flows must at some level be different. As the sperm MTOC appears to be the cue for anterior/posterior polarity at the one-cell stage, centrosomes might function in subsequent anterior/posterior polarity for the lineage of cells that produce the germline; after the first cell division, there is a migration of the nucleus and centrosomes toward the posterior cortex of the germline precursor that precedes cortical flows of both yolk granules (Hird and White, 1993) and NMY-2 and PAR-6 (present study). However, all other early embryonic cells exhibit apicobasal PAR asymmetry, and in these cells there is no obvious relationship between centrosomes/microtubules and the apicobasal axis. Instead, experiments on isolated cells suggest that contacts between cells determine the apicobasal axis (Nance and Priess, 2002). Thus there are likely to be multiple cues that cells can exploit to generate cortical flows, and it will be of interest to see how these converge on the actomyosin cytoskeleton.

### The Anterior PAR Complex Modulates the Cortex to Promote Cortical Flow and Its Own Transport

The fact that depleting embryos of the anterior PAR proteins alters actomyosin dynamics and attenuates cortical flow implies that these proteins are not simply passive cargo transported by an independent flow. It suggests rather that they actively modulate cortical dynamics to promote cortical flow and thus their own transport. The net force acting on the NMY-2 foci must be the sum of active (e.g., contractile) forces that tend to move foci and passive (e.g., viscous and elastic) forces that resist these movements. The deep local furrowing we observe in *par-3* mutants argues against a simple decrease in contractile force generation in *par-3* mutant embryos. An alternative possibility is that the anterior PAR complex could modulate cortical elements that passively resist focus movement, for example by modulating crosslinks within the actomyosin network itself or by modulating other cortical structures that interact mechanically with the actomyosin network to resist its deformation.

### PAR-2 Regulates Establishment and Maintenance of PAR Polarity by Inhibiting the Recruitment of NMY-2 to the Cortex

Studies in several labs suggest that the anterior PAR complex inhibits the association of PAR-2 with the cortex and that depletion of the anterior PAR complex from the posterior cortex removes this inhibition and allows PAR-2 to accumulate there (Cuenca et al., 2003; O'Connell et al., 2000; Rappleye et al., 2002; Severson and Bowerman, 2003; Shelton et al., 1999). PAR-2 in turn is required to maintain the anterior localization of anterior PAR proteins after pseudocleavage in one-cell embryos, but the mechanism by which it acts is unknown (Cuenca et al., 2003). The gap we observe between anterior and posterior PAR domains after pseudocleavage makes it unlikely that PAR-2 acts directly upon members of the anterior PAR complex. Instead, our observations suggest that the loss of anterior PAR asymmetry in *par-2 (RNAi)* embryos is caused by an aberrant flow of NMY-2::GFP and PAR-6::GFP toward the posterior pole that results from the ectopic return of NMY-2 to the posterior cortex after pseudocleavage. Thus we propose that PAR-2 contributes indirectly to maintaining the anterior localization of the anterior PAR complex, by inhibiting recruitment of NMY-2 to the posterior cortex, and thus by preventing inappropriate, NMY-2-driven, flows to the posterior. The same inhibition may also contribute to maintenance of anterior PAR asymmetries by promoting normal anterior-directed flows after pseudocleavage.

However, PAR-2 does not appear to be highly conserved in animal evolution. Thus other mechanisms, including interactions among PAR-1, PAR-5, and the anterior PAR complex (Cuenca et al., 2003; Benton and St Johnston, 2003), or between PAR-1 and NMY-2 (Guo and Kemphues, 1996), must also operate in animals to maintain PAR asymmetries once they are established.

## Experimental Procedures

### Strains

We handled worms as described (Brenner, 1974). We used the following mutant strains: KK571: *par-3(it71) lon-1(e185) /qC1*(Cheng et al., 1995), JJ1320; WH163: *spd-2* (oj29) (O'Connell et al., 2000) KK725: *nop-1(it42)* (Rose et al., 1995). In addition, we used transgenes *zuIs45 (nmy-2::NMY-2::GFP)* (Nance et al., 2003), *zuEx69 (par-6::PAR-6::GFP)* (Nance et al., 2003), and *zuEx121 (pie-1::PAR-6::GFP)* (J.N. and J.R.P., unpublished data).

### Time-Lapse Microscopy

In most experiments, we dissected gravid worms in egg salts (118 mM NaCl, 40 mM KCl, 3.4 mM CaCl, 3.4 mM MgCl, 5 mM HEPES [pH 7.2]) directly on 22 × 22 mm coverslips that we inverted onto 3% agarose pads and sealed with Vaseline. These slightly compressed embryos presented an optimal view of the cortical surface, but we obtained similar results with noncompressed embryos. We viewed embryos at 22–24°C through a 60× 1.4 NA oil immersion lens, using a Biorad Radiance 2000 confocal scanhead mounted on a Nikon E-800 upright scope. We collected a z-series of 5–10 frames per time point. Each frame was a kalman average of three scans at 750 lines/s with: laser transmission set to 12%, confocal aperture = 6, gain = 30, and offset = 0. With these parameters, we could collect over 500 frames without significant photo-bleaching or toxicity. Using custom time-lapse movie software (written by Garry Odell and available on request), we converted each z-series into a single projection, exported it as a jpeg image, and encoded the image sequence as a Quicktime movie.

### Kymograph Analyses

For particle/feature trajectories analysis, we used ImageJ software (http://rsb.info.nih.gov/ij) to extract 512×8 pixel subregions from each image of a time-lapse sequence, then stacked them vertically into single kymograph images. Except where otherwise indicated, we chose subregions aligned with the AP axis, roughly through the center of the egg. We computed speeds from the slopes of kymograph trajectories: particles/features selected for analysis were visible in >5 consecutive frames. Measurements were as follows: particle speed = slope (pixels/frame) * frame rate (frames/second) * length scale (μm/pixel); for relative movement of NMY-2 foci, we used a dimensionless measure: $\Delta d_{30}$ = (final distance – initial distance)/initial distance where the interval between initial and final distance measurements was approximately 30 s (see legend to Supplemental Table S1 for details).

### Immunocytochemistry

Most immunostaining experiments used a standard freeze-crack methanol fixation (Leung et al., 1999). Antibodies and dilutions were as follows: 1:200 chicken anti-GFP (Chemicon), 1:10 mouse anti-HMP-2 (Costa et al., 1998), 1:10 mouse rabbit anti-HMR-1 (Costa et al., 1998), 1:300 rabbit anti-LAD-1 (Chen et al., 2001), 1:50 rabbit anti-NMY-2 (Guo and Kemphues, 1996), 1:50 mouse anti-PAR-3 (Nance et al., 2003), 1:10 rabbit anti-PAR-2 (Boyd et al., 1996). Double stains used Alexa 488- and Cy3-conjugated secondary antibodies. Triple stains used FITC-, Cy3-, and Cy5-conjugated secondary antibodies. DAPI at 0.1 μg/ml was included in the final rinse.

To simultaneously visualize NMY-2 and F-actin in fixed embryos, we used bleach treatment followed by chitinase digestion to remove eggshells as described (Costa et al., 1997), then fixed embryos in 4% formaldehyde, 0.2% gluteraldehyde, 0.1% acrolein (Electron Microscopy Sciences), 0.1 mg/ml lysolecithin (Sigma), 60 mM Pipes, 25 mM HEPES, 10 mM EGTA, 2 mM $MgCl_2$, and 100 mM dextrose for 25 min at RT. We blocked embryos in 5% normal goat serum, 1% bovine serum albumin for 30 min to 1 hr, then stained with primary (rabbit anti-NMY-2 1:50 [Guo and Kemphues, 1996]) and secondary (Cy3 anti-rabbit 1:750) antibodies. For aldehyde-fixed embryos, we extended antibody incubations to about 24 hr at RT and rinses to 2 hr at RT. We included FITC-conjugated phallicidin (1 unit/100 μl; Molecular Probes) with the secondary antibody to label F-actin. We collected all images on the confocal microscope with the exception of Figure 2G, which we collected on a DeltaVision scope and deconvolved as described (Nance et al., 2003).

### RNA-Mediated Interference

We amplified the following sequences from genomic DNA; sequences are numbered relative to the predicted ATG start site of the gene (www.wormbase.org; release WS120):*mlc-4* (219-561); par-1 (17333-18085); *par-2* (6378-7144); *par-3* (6367-7429); *par-6* (2801-4779); *pkc-3* (1971-3190) and *spd-5* (381-1420). We cloned all DNA sequences into the RNAi feeding vector pPD129.36 (ftp://www.ciwemb.edu/pub/FireLabInfo/) and performed RNAi feeding experiments as described (Timmons et al., 2001). We examined embryos after worms had been continuously fed for >24 hr at 25°C, except in the case of *mlc-4 (RNAi)* where we examined embryos either at ~16 hr (weakly depleted embryos) or at >24 hr (strongly depleted embryos) when direct inspection revealed cytokinesis failure (multinucleate eggs) in older broodmates.

### Acknowledgments

We thank Kathryn Baker and Ken Kemphues for the generous gift of PAR-2 and NMY-2 antibodies. We thank members of the Priess lab and the Center for Cell Dynamics, Bruce Bowerman, Bob Goldstein, and several anonymous reviewers for useful comments or discussions during the course of this work. E.M. especially thanks Bruce Bowerman and members of his lab for help in the initial stages of this work. Some of the nematode strains used in this study were provided by the *Caenorhabditis* Genetics Center, which is funded by the NIH National Center for Research Resources (NCRR). J.N. and J.R.P. are supported by the Howard Hughes Medical Institute. E.M. is supported by NIGMS 5P50 GM66050-02.

Received: April 22, 2004
Revised: July 23, 2004
Accepted: July 23, 2004
Published: September 13, 2004

### References

Barros, C.S., Phelps, C.B., and Brand, A.H. (2003). *Drosophila* nonmuscle Myosin II promotes the asymmetric segregation of cell fate determinants by cortical exclusion rather than active transport. Dev. Cell *5*, 829–840.

Benton, R., and St Johnston, D. (2003). *Drosophila* PAR-1 and 14–3-3 inhibit Bazooka/PAR-3 to establish complementary cortical domains in polarized cells. Cell *115*, 691–704.

Boyd, L., Guo, S., Levitan, D., Stinchcomb, D.T., and Kemphues, K.J. (1996). PAR-2 is asymmetrically distributed and promotes association of P granules and PAR-1 with the cortex in *C. elegans* embryos. Development *122*, 3075–3084.

Bray, D., and White, J.G. (1988). Cortical flow in animal cells. Science *239*, 883–888.

Brenner, S. (1974). The genetics of *Caenorhabditis elegans*. Genetics *77*, 71–94.

Cheeks, R.J., Canmaan, J.C., Gabriel, W.N., Meyer, N., Strome, S., and Goldstein, B. (2004). *C. elegans* PAR proteins function by mobilizing and stabilizing asymmetrically localized protein complexes. Curr. Biol. *14*, 851–862.

Chen, L., Ong, B., and Bennett, V. (2001). LAD-1, the *Caenorhabditis elegans* L1CAM homologue, participates in embryonic and gonadal morphogenesis and is a substrate for fibroblast growth factor receptor pathway-dependent phosphotyrosine-based signaling. J. Cell Biol. *154*, 841–855.

Cheng, N.N., Kirby, C.M., and Kemphues, K.J. (1995). Control of

cleavage spindle orientation in *Caenorhabditis elegans*: the role of the genes par-2 and par-3. Genetics *139*, 549–559.

Costa, M., Draper, B.W., and Priess, J.R. (1997). The role of actin filaments in patterning the *Caenorhabditis elegans* cuticle. Dev. Biol. *184*, 373–384.

Costa, M., Raich, W., Agbunag, C., Leung, B., Hardin, J., and Priess, J.R. (1998). A putative catenin-cadherin system mediates morphogenesis of the *Caenorhabditis elegans* embryo. J. Cell Biol. *141*, 297–308.

Cuenca, A.A., Schetter, A., Aceto, D., Kemphues, K., and Seydoux, G. (2003). Polarization of the *C. elegans* zygote proceeds via distinct establishment and maintenance phases. Development *130*, 1255–1265.

Hird, S.N., Paulsen, J.E., and Strome, S. (1996). Segregation of germ granules in living *C. elegans* embryos: cell-type-specific mechanisms for cytoplasmic localization. Development *122*, 1303–1312.

Doe, C.Q., and Bowerman, B. (2001). Asymmetric cell division: fly neuroblast meets worm zygote. Curr. Opin. Cell Biol. *13*, 68–75.

Etemad-Moghadam, B., Guo, S., and Kemphues, K.J. (1995). Asymmetrically distributed PAR-3 protein contributes to cell polarity and spindle alignment in early *C. elegans* embryos. Cell *83*, 743–752.

Goldstein, B., and Hird, S.N. (1996). Specification of the anteroposterior axis in *Caenorhabditis elegans*. Development *122*, 1467–1474.

Guo, S., and Kemphues, K.J. (1995). par-1, a gene required for establishing polarity in *C. elegans* embryos, encodes a putative Ser/Thr kinase that is asymmetrically distributed. Cell *81*, 611–620.

Guo, S., and Kemphues, K.J. (1996). A non-muscle myosin required for embryonic polarity in *Caenorhabditis elegans*. Nature *382*, 455–458.

Hamill, D.R., Severson, A.F., Carter, J.C., and Bowerman, B. (2002). Centrosome maturation and mitotic spindle assembly in *C. elegans* require SPD-5, a protein with multiple coiled-coil domains. Dev. Cell *3*, 673–684.

Hill, D.P., and Strome, S. (1988). An analysis of the role of microfilaments in the establishment and maintenance of asymmetry in *Caenorhabditis elegans* zygotes. Dev. Biol. *125*, 75–84.

Hird, S. (1996). Cortical actin movements during the first cell cycle of the *Caenorhabditis elegans* embryo. J. Cell Sci. *109*, 525–533.

Hird, S.N., and White, J.G. (1993). Cortical and cytoplasmic flow polarity in early embryonic cells of *Caenorhabditis elegans*. J. Cell Biol. *121*, 1343–1355.

Hung, T.J., and Kemphues, K.J. (1999). PAR-6 is a conserved PDZ domain-containing protein that colocalizes with PAR-3 in *Caenorhabditis elegans* embryos. Development *126*, 127–135.

Joberty, G., Petersen, C., Gao, L., and Macara, I.G. (2000). The cell-polarity protein Par6 links Par3 and atypical protein kinase C to Cdc42. Nat. Cell Biol. *2*, 531–539.

Kemphues, K.J., Priess, J.R., Morton, D.G., and Cheng, N.S. (1988). Identification of genes required for cytoplasmic localization in early *C. elegans* embryos. Cell *52*, 311–320.

Kirby, C., Kusch, M., and Kemphues, K. (1990). Mutations in the par genes of *Caenorhabditis elegans* affect cytoplasmic reorganization during the first cell cycle. Dev. Biol. *142*, 203–215.

Leung, B., Hermann, G.J., and Priess, J.R. (1999). Organogenesis of the *Caenorhabditis elegans* intestine. Dev. Biol. *216*, 114–134.

Lin, D., Edwards, A.S., Fawcett, J.P., Mbamalu, G., Scott, J.D., and Pawson, T. (2000). A mammalian PAR-3-PAR-6 complex implicated in Cdc42/Rac1 and aPKC signalling and cell polarity. Nat. Cell Biol. *2*, 540–547.

Nance, J., Munro, E.M., and Priess, J.R. (2003). *C. elegans* PAR-3 and PAR-6 are required for apicobasal asymmetries associated with cell adhesion and gastrulation. Development *130*, 5339–5350.

Nance, J., and Priess, J.R. (2002). Cell polarity and gastrulation in *C. elegans*. Development *129*, 387–397.

Nigon, V., Guerrier, P., and Monin, H. (1960). L'architecture palaire de l'oeuf et les movements des constituants cellulaires au cours des premieres etapes du developpement chez quelques nematodes. Null. Biol. Fr. Belg. *94*, 131–202.

O'Connell, K.F., Maxwell, K.N., and White, J.G. (2000). The spd-2 gene is required for polarization of the anteroposterior axis and formation of the sperm asters in the *Caenorhabditis elegans* zygote. Dev. Biol. *222*, 55–70.

Ohno, S. (2001). Intercellular junctions and cellular polarity: the PAR-aPKC complex, a conserved core cassette playing fundamental roles in cell polarity. Curr. Opin. Cell Biol. *13*, 641–648.

Rappleye, C.A., Paredez, A.R., Smith, C.W., McDonald, K.L., and Aroian, R.V. (1999). The coronin-like protein POD-1 is required for anterior-posterior axis formation and cellular architecture in the nematode *caenorhabditis elegans*. Genes Dev. *13*, 2838–2851.

Rappleye, C.A., Tagawa, A., Lyczak, R., Bowerman, B., and Aroian, R.V. (2002). The anaphase-promoting complex and separin are required for embryonic anterior-posterior axis formation. Dev. Cell *2*, 195–206.

Rose, L.S., Lamb, M.L., Hird, S.N., and Kemphues, K.J. (1995). Pseudocleavage is dispensable for polarity and development in *C. elegans* embryos. Dev. Biol. *168*, 479–489.

Severson, A.F., and Bowerman, B. (2003). Myosin and the PAR proteins polarize microfilament-dependent forces that shape and position mitotic spindles in *Caenorhabditis elegans*. J. Cell Biol. *161*, 21–26.

Shelton, C.A., Carter, J.C., Ellis, G.C., and Bowerman, B. (1999). The nonmuscle myosin regulatory light chain gene mlc-4 is required for cytokinesis, anterior-posterior polarity, and body morphology during *Caenorhabditis elegans* embryogenesis. J. Cell Biol. *146*, 439–451.

Sonneville, R., and Gonczy, P. (2004). zyg-11 and cul-2 regulate progression through meiosis II and polarity establishment in *C. elegans* development. Development *131*, 3527–3543.

Strome, S. (1986). Fluorescence visualization of the distribution of microfilaments in gonads and early embryos of the nematode *Caenorhabditis elegans*. J. Cell Biol. *103*, 2241–2252.

Tabuse, Y., Izumi, Y., Piano, F., Kemphues, K.J., Miwa, J., and Ohno, S. (1998). Atypical protein kinase C cooperates with PAR-3 to establish embryonic polarity in *Caenorhabditis elegans*. Development *125*, 3607–3614.

Timmons, L., Court, D.L., and Fire, A. (2001). Ingestion of bacterially expressed dsRNAs can produce specific and potent genetic interference in *Caenorhabditis elegans*. Gene *263*, 103–112.

Wallenfang, M.R., and Seydoux, G. (2000). Polarization of the anterior-posterior axis of *C. elegans* is a microtubule-directed process. Nature *408*, 89–92.

Watts, J.L., Etemad-Moghadam, B., Guo, S., Boyd, L., Draper, B.W., Mello, C.C., Priess, J.R., and Kemphues, K.J. (1996). par-6, a gene involved in the establishment of asymmetry in early *C. elegans* embryos, mediates the asymmetric localization of PAR-3. Development *122*, 3133–3140.

White, J.G., and Borisy, G.G. (1983). On the mechanisms of cytokinesis in animal cells. J. Theor. Biol. *101*, 289–316.

Wodarz, A. (2002). Establishing cell polarity in development. Nat. Cell Biol. *4*, E39–E44.